INTERNATIONAL JOURNAL FOR NUMERICAL METHODS IN ENGINEERING, VOL. 38, 2929–2949 (1995)

ON AUGMENTED LAGRANGIAN ALGORITHMS FOR THERMOMECHANICAL CONTACT PROBLEMS WITH FRICTION

G. ZAVARISE[1], P. WRIGGERS[2] AND B. A. SCHREFLER[1]

[1]*Istituto di Scienza e Tecnica delle Costruzioni, Via Marzolo 9, 35131 Padova, Italy*
[2]*Institut für Mechanik, Technische Hochschule, Hochschulstr. 1, D-6100 Darmstadt, Germany*

SUMMARY

The detailed discretization of contact zones with contact stiffness based on real physical characteristics of contact surfaces can produce stiffness terms which induce ill-conditioning of the global stiffness matrix. Moreover the consistent treatment of frictional behaviour generates non-symmetric tangent stiffness matrices due to the non-associativity of the slip phase. Other non-symmetries are due to the coupling terms and to the dependencies on various parameters that can be involved. To overcome these difficulties almost consistent techniques based on two-step algorithms have been proposed in the past. Here an augmentation technique is proposed which takes into account micro-mechanical effects, and permits the symmetrization of the tangent stiffness during frictional slip phase.

KEY WORDS: contact; friction; augmentation; thermomechanical coupling

INTRODUCTION

Contact mechanics is a research field that has recently received a strong impulse for the solution of large problems and for the detailed analysis of forces and heat transmission mechanisms. The field can be subdivided into different research areas: the enhancement of the contact search algorithms, the formulation of contact constraints, the linearization of the equation set. Recently microscopical phenomena which take place in the contact zone have also attracted attention.

Several approaches are actually proposed for the numerical treatment of contact constraints.[1–4] Here a formulation is presented dealing with coupling effects between thermal and mechanical fields. The thermomechanical stiffness is based on microscopic mechanisms of force transmission and heat exchange. Using a microscopic approach and combining it with a statistical description of the parameters involved, constitutive laws have been formulated to deal with the normal and tangential contact stiffness, and the thermal contact resistance. In more detail, experimentally and theoretically well-founded micromechanical and microthermal laws have been adapted here to FE discretization. Based on these laws the non-linear macroscopic related stiffnesses are calculated with dependence on changes in significant parameters. For a detailed discussion on the micromechanical approach see References 5–7.

Below, the physical laws are used in contact elements with linear geometry and consistent linearizations of the geometrical and physical terms are carried out. The geometry of the contact is an extended version of the basic one presented in Reference 8.

CCC 0029–5981/95/172929–21

Received 2 December 1993
Revised 17 October 1994

CHARACTERISTICS OF CONTACT LAWS

When taking into account contact phenomena at the microscopic level a general compact form of the normal, tangential and thermal laws in the contact interface Γ_c can be obtained by defining three functions, $\hat{f}_n$, $\hat{f}_t$ and $\hat{f}_h$, as follows:

$$f_n = \hat{f}_n(g_n, A) \tag{1}$$

$$f_t = \hat{f}_t(g_n, g_t, A) \tag{2}$$

$$f_h = \hat{f}_h(g_n, g_t, g_h, t_g, A) \tag{3}$$

where f_n, f_t and f_h denote the normal contact force, the tangential force and the heat flux across the apparent contact area A. Moreover g_n, g_t and g_h denote the mean planes approach which corresponds to the normal displacement, the tangential displacement and the temperature jump across the contact. Finally t_g represents the temperature of the gas inside the microcavities. More details on how to formulate such laws can be found in References 5–7.

Applied to numerical computations, the physical approach leads frequently to stiffness terms which are several orders of magnitude larger than the stiffness terms coming out of the discretization of the solids; hence the global stiffness matrix becomes ill-conditioned and lack of convergence may ensue. For instance, considering the normal contact stiffness for metallic materials, stiffness terms coming out either from micromechanical laws with common surface finishing, or from the necessity to limit unrealistic surface penetrations, assume usually very high values. The problem has been managed using either quadruple precision,[9] or the augmented Lagrangian technique.[10] The latter method permits the analysis to deal with low stiffness parameters which do not correspond to the physical ones. The satisfaction of the constraint conditions is then imposed within an iteration inside the time step. In this iteration the forces due to the contact stiffness are imposed as external ones. When convergence within the step is achieved, the equilibrium is obtained for contact forces imposed as external forces, and the penalty stiffness is not involved anymore, because the relative displacement field in the contact zone is zero (see also References 10–12). The augmentation technique proposed for the micromechanical approach[10] is a modification of the standard procedure. In this case the constraint conditions take into account the real stiffness of the microasperities, and the approach of the mean planes surfaces.

It should be remarked that if the real tangent stiffness matrix is known, the equilibrium iteration has a quadratic rate of convergence near the solution,[9] whereas the augmented Lagrangian iteration has a linear rate of convergence. The theoretical possibility to nest together iteration and augmentation loops is not convenient because the augmented Lagrangian iteration lacks a quadratic rate of convergence.

Considering the frictional behaviour again, numerical problems occur in the stick phase due to the high tangential stiffness. The simple Coulomb's law considers no displacement in this phase, i.e. infinite stiffness. Using a micromechanical model an elastic deformation of the contacting asperities can be considered, but even in this case the tangential stiffness generates ill-conditioning of the global stiffness matrix.

Moreover with Coulomb's law during the slip phase we have no dependence of the tangential forces on the tangential displacement. On the other hand a dependence comes from the normal approach, which modifies the slip limit. The fact that sliding of the surfaces does not produce dilatancy leads to an unsymmetric stiffness matrix. This non-symmetry appears even if more sophisticated dependencies[5,13] are used. The symmetrization of the problem requires an algorithm which assumes no dependence on the normal approach; this means that the iteration loop

should be carried out using a constant normal force, even if the normal force varies. In such a case the tangent stiffness matrix due to friction is zero. This two-step procedure has been used in the past.[3,14]

Also, for the frictional behaviour an augmentation technique can be used to exactly satisfy the theoretical conditions,[15] and in this case too the algorithm can be adapted to impose real physical deformation of the asperities. Moreover, the symmetrization using the two-step technique can also be used within the augmentation loop.[16] Here, a new technique for symmetrization is proposed that seems to give a better rate of convergence.

Within the context of thermomechanical problems the contact thermal resistance usually does not cause numerical problems. The thermal stiffness can be predefined as an input parameter, or computed on a micromechanical base, as reported in References 5 and 6. However, augmentation can be applied also to the thermal relationship.

PROBLEM DEFINITION

We consider two generic bodies B^α ($\alpha = 1, 2$), the associated displacement field $\mathbf{u}^\alpha$, and the temperature fields t^α. The two bodies can have contact along predefined contact zones Γ_c^α.

A general form of the mathematical problem can be obtained by minimization of a functional for the frictionless case which takes into account the continuum and the contact zones. In the case of coupled problems with friction we use the principle of virtual work which leads to $\delta W_M = 0$. The weak form of the heat equation will be denoted by $\delta W_T = 0$. Moreover the contact contribution can be evidenced distinguishing between the continuum part, δW^α, and the contact part, δW^{Γ_c}.

$$\begin{aligned} \delta W_M(\mathbf{u}, t) &= \sum_{\alpha=1}^{2} \delta W_M^\alpha(\mathbf{u}^\alpha, t^\alpha) + \delta W_M^{\Gamma_c}(\mathbf{u}^1, \mathbf{u}^2, t^1, t^2) = 0 \\ \delta W_T(\mathbf{u}, t) &= \sum_{\alpha=1}^{2} \delta W_T^\alpha(\mathbf{u}^\alpha, t^\alpha) + \delta W_T^{\Gamma_c}(\mathbf{u}^1, \mathbf{u}^2, t^1, t^2) = 0 \end{aligned} \tag{4}$$

Of course the contact contribution involves only the part of the boundary where the contact is closed, i.e. the following inequality should be checked:

$$g_n \leqslant \xi \tag{5}$$

where ξ is the initial mean planes distance. This relationship takes into account the microscopic roughness of the surface, and means that the contact is closed when the computed mean planes distance is less than or equal to the initial asperities height. A criterion more often employed, e.g. for the standard penalty approach, is

$$g_n \leqslant 0 \tag{6}$$

which means that contact is active when penetration starts.

AUGMENTED LAGRANGIAN FORMULATION

The augmented Lagrangian technique is a procedure that can be used to avoid ill-conditioning of the global stiffness matrix when constraints are present. It permits the contact conditions to be satisfied while avoiding the use of high penalty values that can occur when limiting undesirable surface penetration or the requirement to impose the real physical stiffness of contact surfaces. Application of this procedure to frictionless contact can be found in Reference 12. Extension to

the frictional case has been more recently proposed.[14,16] Moreover particularization to the microscopical constitutive law for normal stiffness is proposed in Reference 10. Here we focus on the frictional part, with consideration of the microscopical constitutive law and symmetrization of the stiffness matrix.

The augmentation technique with a micromechanical model requires a new constraint condition. If the computation is carried out using a normal stiffness not corresponding to the real one, we have to distinguish between the geometrical approach coming out from the stiffness used for the augmentation loop, g_{n+}, and the real microscopical approach due to the normal contact forces, g_n. The convergence of the augmented loop is hence obtained when the two approaches are equal. It should be remarked that in the standard augmented approach the target value is fixed, no penetration of the surfaces takes place, i.e.

$$g_{n+} = 0 \tag{7}$$

Instead with the micromechanical approach the target value is a function of the pressure, which involves a new non-linearity. Using equation (1) to solve for g_n we can write

$$g_{n+}(\mathbf{u}^1, \mathbf{u}^2) - g_n(f_n, A) = 0 \tag{8}$$

This procedure is described in more detail in Reference 10.

The same method can also be used for the tangential part. Using Coulomb's law the stick phase is governed by a dummy tangential stiffness, and the augmentation loop should move the elastic stick displacement back to zero,

$$g_{t+}(\mathbf{u}^1, \mathbf{u}^2) = 0 \tag{9}$$

Considering a micromechanical law the elastic stick displacement should correspond to the elastic displacement of the microscopic asperities. In such a case using equations (1) and (2) we arrive at

$$g_{t+}(\mathbf{u}^1, \mathbf{u}^2) - g_t(f_t, f_n, A) = 0 \tag{10}$$

When slip takes place equations (9) and (10) are still valid if the slip part of the tangential displacement is removed, see also equation (13).

Finally the activation of the thermal field does not depend on an inequality involving thermal unknowns. It depends on the fact that the gap is open or closed, i.e. on the same inequality that rules the normal contact. The same criteria can be used for the thermal field, but in this case we have to consider the fact that the temperature jump across the contact is different from zero. This means we always have to satisfy a condition like

$$g_{h+}(\mathbf{u}^1, \mathbf{u}^2) - g_h(f_h, f_n, f_t, t_g, A) = 0 \tag{11}$$

The simplest constitutive equation for the real temperature jump g_h could depend on a predefined constant stiffness. However the real physical behaviour requires that g_h should at least depend on the normal force.

The geometrical approach is defined evaluating the distance of two points lying in the normal direction of surfaces Γ_c^1 and Γ_c^2.

$$g_{n+} = \begin{cases} (\mathbf{u}^2 - \mathbf{u}^1)\cdot\mathbf{n} & \text{for } (\mathbf{u}^2 - \mathbf{u}^1)\cdot\mathbf{n} < 0 \\ 0 & \text{for } (\mathbf{u}^2 - \mathbf{u}^1)\cdot\mathbf{n} \geqslant 0 \end{cases} \tag{12}$$

where $\mathbf{n}$ is the normal to the surface Γ_c^2 computed in the projection point.

The tangential displacement is defined by

$$g_{t+} = \begin{cases} (\mathbf{u}^2 - \mathbf{u}^1)\cdot\mathbf{t} - g_{t+}^{slip} & \text{for } g_{n+} \neq 0 \\ 0 & \text{for } g_{n+} = 0 \end{cases} \tag{13}$$

where $\mathbf{t}$ is the tangent unit vector computed in the projection point on Γ_c^2 and g_{t+}^{slip} represents the slip part of the displacement, that has to be removed for stiffness computation.

Finally in the case of a coupled analysis the temperature jump across the contact is defined as

$$g_{h+} = \begin{cases} (t^2 - t^1) & \text{for } g_{n+} \neq 0 \\ 0 & \text{for } g_{n+} = 0 \end{cases} \tag{14}$$

The system of equations defining the problem is then given by the weak forms describing mechanical and thermal behaviour of the bodies, plus constraint conditions for normal, tangential and thermal contact.

$$\delta W_M(\mathbf{u}, t) = \sum_{\alpha=1}^{2} \delta W_M^{\alpha}(\mathbf{u}^{\alpha}, t^{\alpha}) + \delta W_M^{\Gamma_c}(\mathbf{u}^1, \mathbf{u}^2, t^1, t^2) = 0$$

$$\text{subject to } \begin{cases} n_+ = g_{n+} - g_n = 0 \\ t_+ = g_{t+} - g_t = 0 \end{cases}$$

$$\delta W_T(\mathbf{u}, t) = \sum_{\alpha=1}^{2} \delta W_T^{\alpha}(\mathbf{u}^{\alpha}, t^{\alpha}) + \delta W_T^{\Gamma_c}(\mathbf{u}^1, \mathbf{u}^2, t^1, t^2) = 0$$

$$\text{subject to } h_+ = g_{h+} - g_h = 0$$

This set of equations can be used also as a starting point for a formulation of contact without a microscopical contact law. In such a case we simply have to impose

$$g_n = g_t = 0 \tag{16}$$

which means

$$n_+ = g_{n+} \tag{17}$$

$$t_+ = g_{t+} \tag{18}$$

The temperature jump across the contact should be different from zero, as remarked previously, otherwise it means that no thermal contact resistance is involved. Hence the simplest formulation requires the definition of a constant contact thermal conductivity H and leads to

$$f_h = H g_h \tag{19}$$

Then the thermal constraint condition becomes

$$h_+ = g_{h+} - \frac{f_h}{H} = 0 \tag{20}$$

The contact contribution can be expressed using the virtual work of the contact forces. Equation (4) leads then to the augmented Lagrangian formulation

$$\begin{aligned} \delta W_M(\mathbf{u}, t) &= \sum_{\alpha=1}^{2} \delta W_M^{\alpha}(\mathbf{u}^{\alpha}, t^{\alpha}) + \int_{\Gamma_c} (p_n \delta g_{n+} + p_t \delta g_{t+})\, d\Gamma + \int_{\Gamma_c} (\varepsilon n_+ \delta g_{n+} + \chi t_+ \delta g_{t+})\, d\Gamma = 0 \\ \delta W_T(\mathbf{u}, t) &= \sum_{\alpha=1}^{2} \delta W_T^{\alpha}(\mathbf{u}^{\alpha}, t^{\alpha}) + \int_{\Gamma_c} p_h \delta g_{h+}\, d\Gamma + \int_{\Gamma_c} \gamma h_+ \delta g_{h+}\, d\Gamma = 0 \end{aligned} \tag{21}$$

ε, χ and γ represent normal, tangential and thermal penalty parameters, respectively, used within the augmentation loop. The first integral represents the virtual work of the augmented forces, p_n, p_t and p_h, which are assumed to be known for the moment. The second one represents the virtual work due to the penalty stiffness.

The equilibrium iteration within the step can be carried out by updating the augmented forces at each iteration. In such a way we obtain only a linear rate of convergence. It is usually more effective to split augmentation and iteration loops within the time step. Then, the equations within a time step are solved using an external augmentation loop. Equilibrium iterations, with a quadratic rate of convergence, are carried out after each augmentation.

The new set of augmented forces is computed as follows:

$$p_n^{t+1\,a+1} = p_n^{t+1\,a} + \varepsilon n_+^{t+1\,i}_{a} \tag{22}$$

$$p_t^{t+1\,a+1} = p_t^{t+1\,a} + \chi t_+^{t+1\,i}_{a} \tag{23}$$

$$p_h^{t+1\,a+1} = p_h^{t+1\,a} + \gamma h_+^{t+1\,i}_{a} \tag{24}$$

where the current status is identified by time step $t+1$, augmentation $a+1$ and iteration $i+1$. We have to remark that n_+, t_+ and h_+ are non-linear functions; thus the update procedure is different from the standard one.[11]

The updating scheme for the constraint condition for the iteration $i+1$ is the following:

$$n_+^{t+1\,i+1}_{a+1} = g_{n+}^{t+1\,i+1}_{a+1} - g_n^{t+1\,a+1} \tag{25}$$

$$t_+^{t+1\,i+1}_{a+1} = g_{t+}^{t+1\,i+1}_{a+1} - g_t^{t+1\,a+1} \tag{26}$$

$$h_+^{t+1\,i+1}_{a+1} = g_{h+}^{t+1\,i+1}_{a+1} - g_h^{t+1\,a+1} \tag{27}$$

We remark that the update criterion considers the physical approach target value as a constant within iterations. New target values are determined at each augmentation.

The fully coupled system of equation (21) leads to a non-symmetric tangent operator when linearized. This is due to the coupling terms, and to dependencies on geometrical and thermal quantities, see e.g. References 5, 6 and 13.

It has been proved that for some classes of coupled problems it may be effective to employ a staggered procedure.[17] In such cases the coupling terms disappear, and it would be interesting to check the possibility to symmetrize the problem entirely. Disregarding coupling terms we still have a non-symmetric formulation. The first cause is the dependence of (1)–(3) on the apparent area. This effect only occurs when large deformations are present,[5] but it has a limited influence, see Reference 18, and thus can be disregarded. Another cause is associated with the gas temperature which affects the heat exchange through the gas in the microcavities.[19] Also this influence is very small and can be neglected. The most significant cause is due to the influence of

normal forces on the tangential force during the slip phase. Some techniques are available in the literature to symmetrize these dependencies.[14,16]

The basic technique of symmetrization of the frictional equation set during the slip phase considers a different update scheme for the normal contact force and the normal force used to compute the frictional slip limit. Using a consistent approach the normal force is computed within the iteration to check if the slip limit has been reached,

$$\overset{i+1}{\underset{a+1}{f^{t+1}_{t\max}}} = F(\overset{i+1}{\underset{a+1}{f^{t+1}_{n}}}) \tag{28}$$

Here the generic function F has been particularized for Coulomb's law using the constant friction coefficient μ,

$$\overset{i+1}{\underset{a+1}{f^{t+1}_{t\max}}} = \mu \overset{i+1}{\underset{a+1}{f^{t+1}_{n}}} \tag{29}$$

In the case of the standard procedure without augmentation the previous relationship yields

$$f^{t+1}_{t\max} = \mu f^{t+1}_{n} \tag{30}$$

This relationship implies a dependence on the current normal approach, and then the unsymmetric terms appear. To avoid it a so-called two-step algorithm was proposed in Reference 14 in the case of no augmentation. The method solves the frictional behaviour using not the current normal force but the normal force of one step behind,

$$f^{t+1}_{t\max} = \mu f^{t}_{n} \tag{31}$$

Of course this strategy affects the rate of convergence. It can also be used in the case of the augmentation technique, i.e.

$$\overset{i+1}{a+1}\, f^{t+1}_{t\max} = \mu f^{t}_{n} \tag{32}$$

More recently a different technique has been proposed in Reference 16. Considering that the augmentation loop is nested inside the time step loop, and that usually the augmented step is an equilibrated one, it can be used as a 'more recent' solution point for the normal force.

$$\overset{i+1}{a+1}\, f^{t+1}_{t\max} = \mu \overset{a}{f^{t+1}_{n}} \tag{33}$$

In this procedure the pressure used for determining the maximum admissible tangential force lags one augmentation step behind the current status. Both these choices imply that the first solution phase is frictionless. However it can be shown that if the first augmentation is frictionless then some difficulties arise in the second one, due to the sudden change in the tangential force. This fact can destabilize the solution and may lead in some cases to divergence.

The crucial point for symmetrization is that when the slip takes place we have to use a constant normal force for computing the slip limit. It could be reasonable to use a "more recent" normal force instead of the normal force of the previous augmentation.

To use a more recent value for the normal force, probably nearer to the solution value, we propose to take the last value available in the iteration loop. This means that when the slip occurs we compute the maximum allowable tangential force, and then keep the value constant for the remaining iterations.

$$f_{\mathrm{tmax}}^{\substack{t+1\\a+1}} = \mu f_{\mathrm{n}}^{\substack{\bar{i}\\a+1}} \tag{34}$$

where $\bar{i}$ is the iteration value at which slip started. Examples have shown good results, and convergence was achieved also for cases where the other algorithms failed.

FINITE ELEMENT FORMULATION

The finite element model can be formulated within a general framework for large deformations;[5] however we restrict ourselves to the case of small strains and displacements to focus on the basic algorithm features. We therefore extend the simple element used in References 10 and 19. In the case of contact surfaces being parallel to the x-axis we have

$$g_{\mathrm{n}+} = y_2 - y_1 = (Y_2 + v_2) - (Y_1 + v_1) \tag{35}$$

where Y, v and y denote the initial vertical position, the current vertical displacement and the current vertical position of the node, respectively. By defining vectors $\mathbf{U}_e$ containing the current node position and vectors $\mathbf{N}, \mathbf{T}, \mathbf{H}$, containing constant coefficients

$$\mathbf{U}_e = \begin{bmatrix} X_1 + u_1 \\ Y_1 + v_1 \\ T_1 + t_1 \\ X_2 + u_2 \\ Y_2 + v_2 \\ T_2 + t_2 \end{bmatrix}, \quad \mathbf{N} = \begin{bmatrix} 0 \\ -1 \\ 0 \\ 0 \\ 1 \\ 0 \end{bmatrix}, \quad \mathbf{T} = \begin{bmatrix} -1 \\ 0 \\ 0 \\ 1 \\ 0 \\ 0 \end{bmatrix}, \quad \mathbf{H} = \begin{bmatrix} 0 \\ 0 \\ -1 \\ 0 \\ 0 \\ 1 \end{bmatrix} \tag{36}$$

we can write equation (12) as

$$g_{\mathrm{n}+} = \mathbf{U}_e^{\mathrm{T}}\mathbf{N} \tag{37}$$

In a similar way we obtain from equations (13) and (14)

$$g_{\mathrm{t}+} = \mathbf{U}_e^{\mathrm{T}}\mathbf{T} - g_{\mathrm{t}+}^{\mathrm{slip}} \tag{38}$$

$$g_{\mathrm{h}+} = \mathbf{U}_e^{\mathrm{T}}\mathbf{H} \tag{39}$$

Using equations (4), (21) and (37)–(39) we express the contact contributions of the active contact elements as follows:

$$\int_{\Gamma_c} (p_{\mathrm{n}} + \varepsilon n_+)\delta g_{\mathrm{n}+}\, \mathrm{d}\Gamma = \bigcup_{c=1}^{n_c} [\delta \mathbf{U}_e^{\mathrm{T}}(p_{\mathrm{n}} + \varepsilon n_+)A]_c \mathbf{N} \tag{40}$$

$$\int_{\Gamma_c} (p_{\mathrm{t}} + \chi t_+)\delta g_{\mathrm{t}+}\, \mathrm{d}\Gamma = \bigcup_{c=1}^{n_c} [\delta \mathbf{U}_e^{\mathrm{T}}(p_{\mathrm{t}} + \chi t_+)A]_c \mathbf{T} \tag{41}$$

$$\int_{\Gamma_c} (p_{\mathrm{h}} + \gamma h_+)\delta g_{\mathrm{h}+}\, \mathrm{d}\Gamma = \bigcup_{c=1}^{n_c} [\delta \mathbf{U}_e^{\mathrm{T}}(p_{\mathrm{h}} + \gamma h_+)A]_c \mathbf{H} \tag{42}$$

where n_c is the number of contact elements, A is the element area and $\bigcup$ represents an operator that selects and suitably assembles only the active (closed) element contributions.

The discretization of the continuum problem can be represented in a general form[20] as

$$\sum_{\alpha=1}^{2} \delta W_{\mathrm{M}}^{\alpha}(\mathbf{u}^{\alpha}, t^{\alpha}) = \delta \mathbf{U}^{\mathrm{T}} \mathbf{M}(\mathbf{u}, t) \tag{43}$$

$$\sum_{\alpha=1}^{2} \delta W_{\mathrm{T}}^{\alpha}(\mathbf{u}^{\alpha}, t^{\alpha}) = \delta \mathbf{U}^{\mathrm{T}} \mathbf{T}(\mathbf{u}, t) \tag{44}$$

Equations (40)–(44) permit one to obtain the discretized form of the global problem given by equation (21). This leads, for arbitrary virtual quantities $\delta\mathbf{U}$, to the vector equations

$$\begin{gathered} \mathbf{M}(\mathbf{u}, t) + \bigcup_{c=1}^{n_c} [(p_{\mathrm{n}} + \varepsilon n_+)A]_c \mathbf{N} + \bigcup_{c=1}^{n_c} [\delta \mathbf{U}_e^{\mathrm{T}}(p_{\mathrm{t}} + \chi t_+)A]_c \mathbf{T} = \mathbf{0} \\ \mathbf{T}(\mathbf{u}, t) + \bigcup_{c=1}^{n_c} [(p_{\mathrm{h}} + \gamma h_+)A]_c \mathbf{H} = \mathbf{0} \end{gathered} \tag{45}$$

The algorithmic treatment of the problem requires the linearization of the equation set (4). From the contact contribution in matrix form (equations (40)–(42)) and the chosen contact geometry we obtain the contact tangent stiffness contributions. The normal contact gives

$$\begin{aligned} \Delta\left[\int_{\Gamma_c} (p_{\mathrm{n}} + \varepsilon n_+)\delta g_{\mathrm{n}+}\, \mathrm{d}\Gamma\right] = \bigcup_{c=1}^{n_c} [&\Delta\delta \mathbf{U}_e^{\mathrm{T}}(p_{\mathrm{n}} + \varepsilon n_+)A + \delta \mathbf{U}_e^{\mathrm{T}}(\Delta p_{\mathrm{n}} + \Delta\varepsilon n_+ + \varepsilon \Delta n_+)A \\ &+ \delta \mathbf{U}_e^{\mathrm{T}}(p_{\mathrm{n}} + \varepsilon n_+)\Delta A]_c \mathbf{N} \end{aligned} \tag{46}$$

Due to the chosen contact element geometry and to the solution scheme p_{n}, ε and A are constants. Disregarding second-order terms and using equations (25) and (37) to express n_+ we obtain

$$\bigcup_{c=1}^{n_c} [\delta \mathbf{U}_e^{\mathrm{T}} \varepsilon \Delta n_+ A]_c \mathbf{N} = \bigcup_{c=1}^{n_c} [\delta \mathbf{U}_e^{\mathrm{T}} \varepsilon \Delta g_{\mathrm{n}+} A]_c \mathbf{N} = \bigcup_{c=1}^{n_c} [\delta \mathbf{U}_e^{\mathrm{T}} \varepsilon (\Delta \mathbf{U}_e^{\mathrm{T}} \mathbf{N}) A]_c \mathbf{N} \tag{47}$$

Rearrangement of equation (47) permits to obtain the tangent stiffness matrix

$$\bigcup_{c=1}^{n_c} [\delta \mathbf{U}_e^{\mathrm{T}} (\varepsilon A \mathbf{N}\mathbf{N}^{\mathrm{T}}) \Delta \mathbf{U}_e]_c \Rightarrow \mathbf{K}_{\mathrm{Tn}} = \bigcup_{c=1}^{n_c} (\varepsilon A \mathbf{N}\mathbf{N}^{\mathrm{T}})_c \tag{48}$$

The frictional contribution depends on the current status: in the stick phase the tangential slip, $g_{\mathrm{t}}^{\mathrm{slip}}$, is zero, and the linearization carried out following the same guidelines of the previous one yields

$$\Delta\left[\int_{\Gamma_c} (p_{\mathrm{t}} + \chi t_+)\delta g_{\mathrm{t}+}\, \mathrm{d}\Gamma\right] \Rightarrow \mathbf{K}_{\mathrm{Tt}}^{\mathrm{stick}} = \bigcup_{c=1}^{n_c} (\chi A \mathbf{T}\mathbf{T}^{\mathrm{T}})_c \tag{49}$$

In the slip phase a dependence on the normal force appears. Using Coulomb's law this can simply be evidenced in the following way:

$$g_{\mathrm{t}+} = \frac{f_{\mathrm{t}}}{\chi} = \frac{\mu f_{\mathrm{n}}}{\chi} = \frac{\mu\varepsilon}{\chi} g_{\mathrm{n}+} \tag{50}$$

With equation (50) the linearized form of equation (41) is

$$\Delta\left[\int_{\Gamma_c} (p_{\mathrm{t}} + \chi t_+)\delta g_{\mathrm{t}+}\, \mathrm{d}\Gamma\right] = \int_{\Gamma_c} (\mu\varepsilon \Delta t_+ \delta g_{\mathrm{n}+})\mathrm{d}\Gamma \Rightarrow \mathbf{K}_{\mathrm{Tt}}^{\mathrm{slip}} = \bigcup_{c=1}^{n_c} (\mu A \mathbf{T}\mathbf{N}^{\mathrm{T}})_c \tag{51}$$

Finally the linearized form of the thermal contribution is

$$\Delta\left[\int_{\Gamma_c} (p_{\mathrm{h}} + \gamma h_+)\delta g_{\mathrm{h}+}\, \mathrm{d}\Gamma\right] \Rightarrow \mathbf{K}_{\mathrm{Th}} = \bigcup_{c=1}^{n_c} (\gamma A \mathbf{H}\mathbf{H}^{\mathrm{T}})_c \tag{52}$$

The algorithm is described in detail in Box 1.

Box 1. Scheme of the algorithm

Initialize algorithm
set initial values
LOOP over time step: $t = 1, \ldots,$ *total load condition*
  LOOP over augmentations: $a = 1, \ldots,$ *convergence*
    LOOP over iterations: $i = 1, \ldots,$ *convergence*
      solve

$$\bar{\mathbf{M}} = \mathbf{M}(\overset{i+1}{\underset{a+1}{\mathbf{u}}}{}^{t+1}, \overset{i+1}{\underset{a+1}{t}}{}^{t+1}) + \bigcup_{c=1}^{n_c} \delta\mathbf{U}^{\mathrm{T}}[(\overset{a+1}{p_{\mathrm{n}}}{}^{t+1} + \varepsilon \overset{i+1}{\underset{a+1}{n_+}}{}^{t+1})A\mathbf{N} + (\overset{a+1}{p_{\mathrm{n}}}{}^{t+1} + \chi \overset{i+1}{\underset{a+1}{n_+}}{}^{t+1})A\mathbf{T}] = 0$$

$$\bar{\mathbf{T}} = \mathbf{T}(\overset{i+1}{\underset{a+1}{\mathbf{u}}}{}^{t+1}, \overset{i+1}{\underset{a+1}{t}}{}^{t+1}) + \bigcup_{c=1}^{n_c} \delta\mathbf{U}^{T}(\overset{a+1}{p_{\mathrm{h}}}{}^{t+1} + \gamma \overset{i+1}{\underset{a+1}{h_+}}{}^{t+1})A\mathbf{H} = 0$$

      fulfilling constraint conditions (8),(10),(11)
      check for convergence: $\|\bar{\mathbf{M}} + \bar{\mathbf{T}}\| \leqslant TOL \Rightarrow$ *convergence*
    END LOOP
    LOOP over contact elements: $k = 1, n$
      update augmented forces:

$$\overset{a+1}{p_{\mathrm{n}}}{}^{t+1} = \overset{a}{p_{\mathrm{n}}}{}^{t+1} + \varepsilon \overset{i}{\underset{a}{n_+}}{}^{t+1} \quad \overset{a+1}{p_{\mathrm{t}}}{}^{t+1} = \overset{a}{p_{\mathrm{t}}}{}^{t+1} + \chi \overset{i}{\underset{a}{t_+}}{}^{t+1} \quad \overset{a+1}{p_{\mathrm{h}}}{}^{t+1} = \overset{a}{p_{\mathrm{h}}}{}^{t+1} + \gamma \overset{i}{\underset{a}{h_+}}{}^{t+1}$$

      update physical approaches:
      IF standard way:

$$\overset{a+1}{g_{\mathrm{n}}}{}^{t+1} = g_{\mathrm{n}}(\overset{i}{\underset{a}{f_{\mathrm{n}}}}{}^{t+1}, A) \quad \overset{a+1}{g_{\mathrm{t}}}{}^{t+1} = g_{\mathrm{t}}(\overset{i}{\underset{a}{f_{\mathrm{t}}}}{}^{t+1}, \overset{i}{\underset{a}{f_{\mathrm{n}}}}{}^{t+1}, A)$$

$$\overset{a+1}{g_{\mathrm{h}}}{}^{t+1} = g_{\mathrm{h}}(\overset{i}{\underset{a}{f_{\mathrm{h}}}}{}^{t+1}, \overset{i}{\underset{a}{f_{\mathrm{n}}}}{}^{t+1}, \overset{i}{\underset{a}{f_{\mathrm{t}}}}{}^{t+1}, \overset{i}{\underset{a}{t_{\mathrm{g}}}}{}^{t+1}, A)$$

      ELSE IF symmetric way without thermal field:[16]

$$\overset{a+1}{g_{\mathrm{n}}}{}^{t+1} = g_{\mathrm{n}}(\overset{i}{\underset{a}{f_{\mathrm{n}}}}{}^{t+1}, A) \quad \overset{a+1}{g_{\mathrm{t}}}{}^{t+1} = g_{\mathrm{t}}(\overset{i}{\underset{a}{f_{\mathrm{t}}}}{}^{t+1}, \overset{a}{f_{\mathrm{n}}}{}^{t+1}, A)$$

      ELSE IF proposed way

$$\overset{a+1}{g_{\mathrm{n}}}{}^{t+1} = g_{\mathrm{n}}(\overset{i}{\underset{a}{f_{\mathrm{n}}}}{}^{t+1}, A) \quad \overset{a+1}{g_{\mathrm{t}}}{}^{t+1} = g_{\mathrm{t}}(\overset{i}{\underset{a}{f_{\mathrm{t}}}}{}^{t+1}, \overset{\bar{i}}{\underset{a}{f_{\mathrm{n}}}}{}^{t+1}, A)$$

$$\overset{a+1}{g_{\mathrm{h}}}{}^{t+1} = g_{\mathrm{h}}(\overset{i}{\underset{a}{f_{\mathrm{h}}}}{}^{t+1}, \overset{a}{f_{\mathrm{n}}}{}^{t+1}, \overset{a}{f_{\mathrm{t}}}{}^{t+1}, \overset{a}{t_{\mathrm{g}}}{}^{t+1}, A)$$

      ENDIF
      check constraint condition:

$$\left\| \overset{a+1}{n_+}{}^{t+1} + \overset{a+1}{t_+}{}^{t+1} + \overset{a+1}{h_+}{}^{t+1} \right\| \leqslant TOL \Rightarrow \text{convergence}$$

    END LOOP
  END LOOP
END LOOP

EXAMPLES

The numerical computations have been carried out to demonstrate the influence of different contact features. To do this we decided to focus on the contact mechanics; thus we have eliminated non-linearities within the continuum formulation and have used simple tests with geometrically linear behaviour.

The elastic block on a rigid foundation is a widely used test example for these purposes.[21] The test considers a block 4 units wide and 2 units high (Figure 1). Idealized mechanical parameters often used for the block are: elastic modulus $E = 1000$ *force/length*^{2} and Poisson's coefficient $\nu = 0{\cdot}3$. These parameters characterize a very deformable continuum medium. We have carried out a series of numerical tests using these data. Furthermore some other results have been obtained using the more realistic compression modulus of steel.

The block is discretized by using four-node isoparametric elements in the plane stress condition. Contact features have been studied using penalty as well as micromechanical normal stiffness[5-7] methods. Frictional effects have been included using a penalty stiffness in the normal direction with Coulomb's law or normal and tangential micromechanical stiffnesses. Furthermore, augmentation techniques have been applied to these four cases. All data involved in the description of the contact interface are collected in Table I. Such data can be obtained from measurements of the microscopical surface shape and hardness tests, see e.g. Reference 22.

Compared to the basic example[21] some modifications have been introduced concerning the boundary conditions. Frictional effects are applied all along the contact area and either the vertical load or the imposed displacement at the top are applied along the entire upper edge of the block (see Figure 1).

In the first series of tests a uniform vertical displacement of 0·32 has been applied. The energy tolerance to stop equilibrium iterations within the augmentation loop has been set to $1e-25$ which denotes the limit in double precision computations due to round-off errors. In such a way the order of magnitude of the minimum value obtainable for the residual norm is $1e-12$.

Results of the first four tests (nos. 1, 2, 3, 4 in Table I) are collected in Table II. It is evident in these examples that the frictional effects have a small influence on the rate of convergence. The micromechanical contact law, reported in Figures 2 and 3, is strongly non-linear; hence more

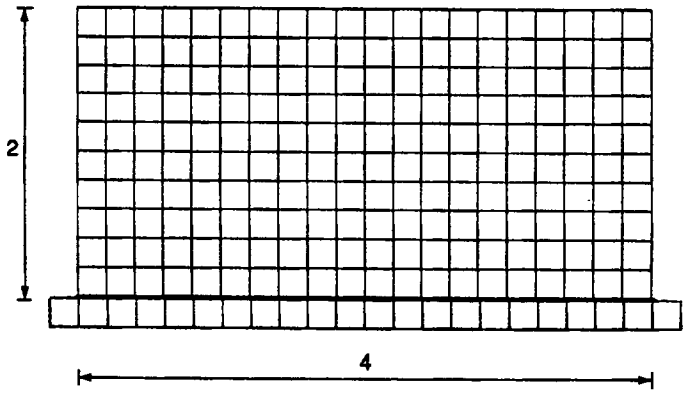

Figure 1. Discretization of the elastic block on rigid foundation

Table I. Contact parameters of the examples

N	Features	Value
1	*Frictionless penalty*	
	Normal penalty	1e + 10
2	*1 + Coulomb's friction*	
	Normal penalty	1e + 10
	Tangential penalty	1e + 10
	Coulomb's friction coefficient	0·1
3	*Frictionless micromechanical*	
	Mean RMS surface roughness	4·78e − 7
	Mean equivalent absolute slope	0·072
	Hardness parameter C1	6·271e + 6
	Hardness parameter C2	− 0·229
4	*3 + micromechanical friction*	
	Tangential elastic stiffness	1e + 7
	Initial shear strength	0
	Final shear strength	0
	Initial coefficient of microfriction	0·1
	Final coefficient of microfriction	0·1
	Hardening exponential constant	0
	Hardening linear constant	0
5	*1 with augmentation*	
	Target stiffness	∞
	Augmentation penalty	1e + 4 ÷ 1e + 6
	Penalty increment ratio	1 ÷ 10
6	*2 with augmentation*	
	Target normal stiffness	1e + 7
	Target tangential stiffness	1e + 7
	Augmentation normal penalty	1e + 5
	Augmentation tangential penalty	1e + 2
	Tangential penalty increment ratio	1 ÷ 2
7	*3 with augmentation*	
	Non-linear target stiffness	0 ÷ 4e + 11
	Augmentation penalty	1e + 4 ÷ 1e + 6
	Penalty increment ratio	1 ÷ 10
8	*4 with augmentation*	
	Non-linear target normal stiffness	0 ÷ 4e + 11
	Non-linear target tangential stiffness	0 ÷ 4e + 11
	Augmentation normal penalty	1e + 9
	Augmentation tangential penalty	1e + 4 ÷ 1e + 6

iterations have to be performed to achieve convergence. However, the rate of convergence near the solution point is quadratic due to consistent linearization (Figure 4).

Within the augmentation technique it is important to determine the proper value of the penalty term. If it is chosen too low then the convergence rate is very poor. Comparisons for different values of the penalty parameter in test no. 5, see Table I, can be deduced from the results collected in Table III. The case of penalty without friction has been tested by varying the penalty parameter

Table II. Residual norm for test nos. 1, 2, 3 and 4

1	2	3	4
0·156e + 4	0·156e + 4	0·156e + 4	0·156e + 4
0·167e − 11	0·990e + 1	0·664e + 6	0·685e + 6
0·416e − 12	0·471e + 1	0·224e + 5	0·224e + 5
—	0·401e − 12	0·759e + 4	0·759e + 4
—	—	0·260e + 4	0·260e + 4
—	—	0·876e + 3	0·876e + 3
—	—	0·276e + 3	0·276e + 3
—	—	0·710e + 2	0·711e + 2
—	—	0·101e + 2	0·131e + 2
—	—	0·311e + 0	0·242e + 1
—	—	0·322e − 3	0·139e − 2
—	—	0·344e − 9	0·912e − 8
—	—	0·486e − 12	0·186e − 10

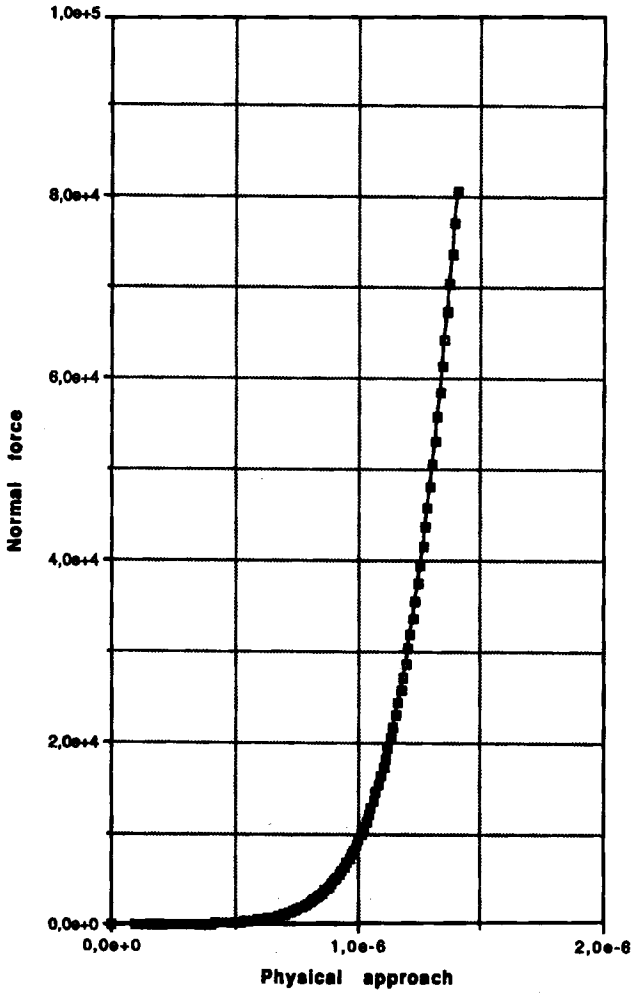

Figure 2. Normal contact force versus physical approach

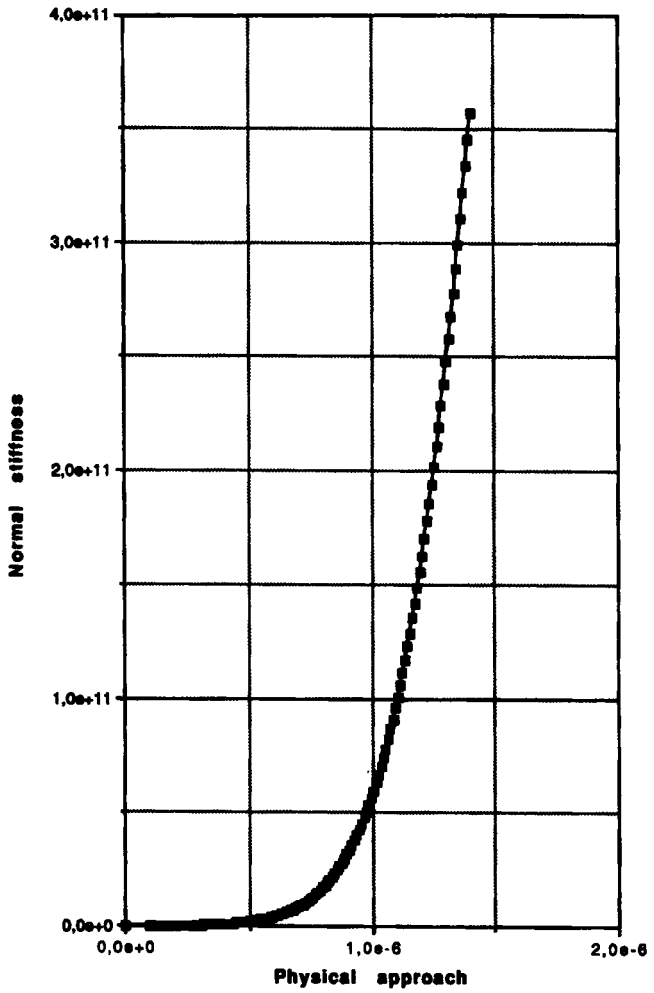

Figure 3. Normal contact stiffness versus physical approach

during the augmentations. Table III depicts the residuals of the constraints during the augmentation loop and the number of iterations required to achieve convergence at each augmentation step. The final penetration obtained is 1e − 17 which is a very good approximation. Note that the computational effort depends strongly on the value selected for the penalty parameter.

The possibility to increase the initial penalty value within an augmentation loop may lead to a better rate of convergence. Unfortunately it is not a simple task to establish a good strategy for increasing the penalty value and for stopping this process at a certain level. Some preliminary results on the choice of the penalty parameter are reported in Wriggers and Nour-Omid.[23] Thus this is a field in which some efforts should be spent, because until now there are no well-set criteria. However as argued from a comparison of the reported results the augmentation technique is really advantageous. To increase the penalty means to disturb somehow the solution process. Hence it can be done only during the first augmentations. The criterion adopted here stops the increment when the maximum admissible value, as stated in Reference 23, is reached, or

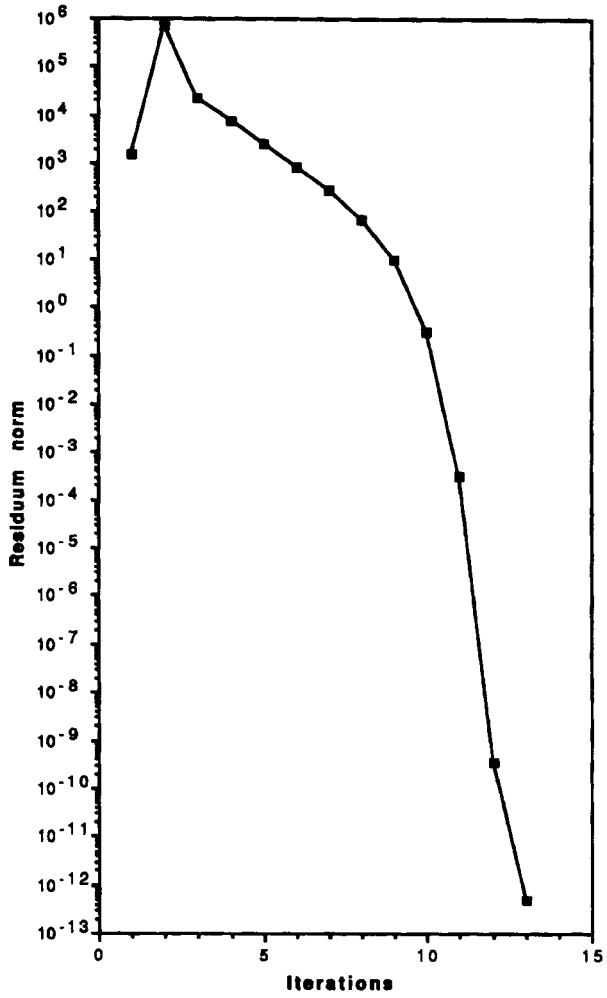

Figure 4. Convergence rate for test no. 3 of Table I

when the ratio between the previous and the current approach is less than 0·25. This criterion allows only one increment at the first augmentation in each test. The effect of the penalty value used for augmentations on the normal approach is shown in Figure 5.

The group of examples no. 6 of Table I are similar to the ones in group no. 2, but here the augmentation technique has been applied to improve the results of normal and tangential contact effects. Due to the chosen contact parameters and load conditions, slip is activated in the main part of the contact zone. Hence the unsymmetric terms in contact tangent matrix strongly influence the solution. Comparisons of different solution strategies are reported in Table IV. The examples show a certain sensitivity to the contact parameters. Many difficulties come from the jumps of tangential forces during augmentations. These jumps determine sometimes the gap opening in certain zones; due to this the solution does not converge. This effect takes place when using a symmetrization technique proposed in References 14 and 16, where the first augmentation is frictionless, then in the second augmentation a big jump in the contact forces occurs. To avoid

Table III. Residual of constraints and number of iterations for test no. 5

Penalty 1e + 4 no increment	Penalty 1e + 5 no increment	Penalty 1e + 6 no increment	Penalty 1e + 4 increment 10	Penalty 1e + 5 increment 10	Penalty 1e + 6 increment 10
3	3	3	3	3	3
0·698e − 1	0·730e − 2	0·733e − 3	0·698e − 1	0·730e − 2	0·733e − 3
2	2	2	2	2	2
0·336e − 2	0·363e − 4	0·366e − 6	0·347e − 3	0·365e − 5	0·366e − 7
2	2	2	2	2	2
0·158e − 3	0·181e − 6	0·183e − 9	0·173e − 5	0·182e − 8	0·183e − 11
2	2	2	2	2	2
0·754e − 5	0898e − 9	0·915e − 13	0·860e − 8	0·911e − 12	0·916e − 16
2	2	2	2	2	—
0·369e − 6	0·447e − 11	0·457e − 16	0·428e − 10	0·455e − 15	—
2	2	—	2	—	—
0·171e − 7	0·222e − 13	—	0·213e − 12	—	—
2	2	—	2	—	—
0·814e − 9	0·111e − 15	—	0·106e − 14	—	—
2	—	—	2	—	—
0·388e − 10	—	—	0·533e − 17	—	—
2	—	—	—	—	—
0·185e − 11	—	—	—	—	—
2	—	—	—	—	—
0·879e − 13	—	—	—	—	—
2	—	—	—	—	—
0·418e − 14	—	—	—	—	—
2	—	—	—	—	—
0·197e − 15	—	—	—	—	—
Tot. iterations					
25	15	11	17	11	9

gap opening a suitable combination of normal and tangential penalty parameters should be chosen. An alternative way can be the use of an active set strategy, which permits traction forces in contact zones during the iterations. Then the solution can be obtained even if the contact forces oscillate with changing sign. The main problem using this strategy is that it is not easy to determine if the contact opening is the correct solution or if it is due to oscillations of contact forces.

The results reported in Table IV show that the convergence rate is quite slow without increase of the tangential contact stiffness. In this case the unsymmetric formulation, the symmetric one proposed in Reference 16 or the one proposed by us give about the same efficiency. With a higher tangential stiffness the problem does not converge due to the opening of some contact elements within the iterations. The effectiveness of the proposed symmetrization is evidenced when an increase of the penalty parameter is adopted. In this case the low starting value avoids gap opening during the first augmentation. Then the increase of the penalty parameter improves the convergence rate. In fact, using the same number of iterations in the case without a tangential penalty increase we are able to fulfil the constraint up to 0·315e − 10 instead of 0·127e − 5. Moreover in this case the proposed symmetrization technique presents almost the same convergence rate as the unsymmetric one. Considering the number of iterations within the augmenta-

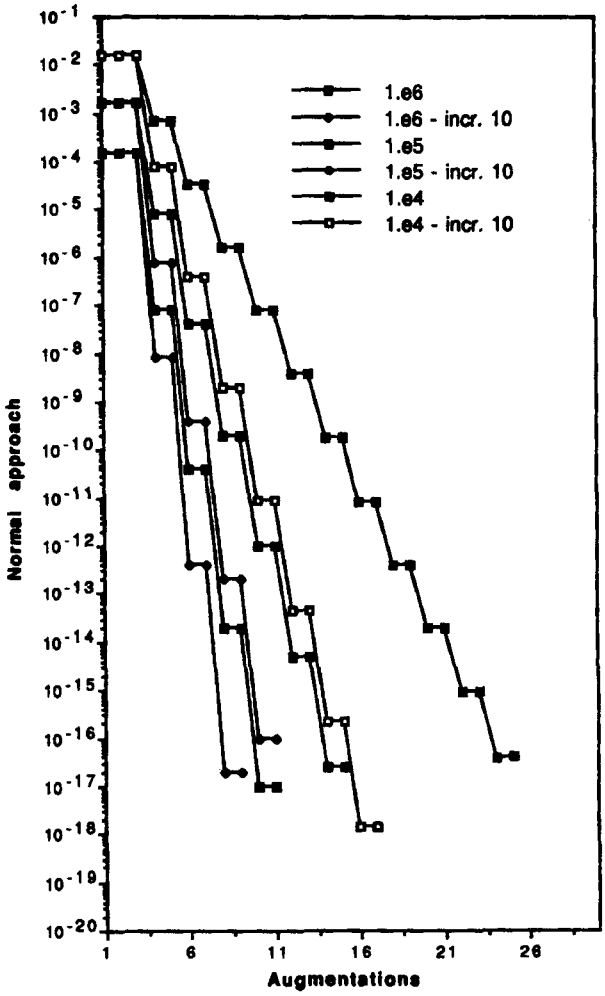

Figure 5. Normal approach with augmentations for test group no. 5

tions the proposed symmetrization also seems to be less sensitive than the other one with respect to the disturbance induced by the update of the penalty parameter.

The effectiveness of the augmentation technique with a micromechanical contact law has been demonstrated in Reference 10. Test no. 7, for which the results are reported in Table V, considers a frictionless contact with micromechanical contact law. The decrease of the residual of the constraints also shows in this case the necessity to increase the penalty stiffness. Due to the micromechanical law the target value for the approach is not zero, but is a variable which evolves during the simulation (see also Reference 10). The final target value for the physical penetration is 4e − 7. Also in this set of tests the algorithm has permitted only one increase of the penalty during the first augmentation.

Test no. 8 collects examples of contact with friction based on a micromechanical contact law. The augmentation technique is used for both normal and frictional contact behaviour. The efficiency of the proposed technique to symmetrize the contact stiffness matrix during the slip

Table IV. Residual of constraints and number of iterations for test no. 6

Target stiffness: normal 1e + 7, tangential 1e + 7					
Normal penalty 1e + 5 Tangential penalty 1e + 2			Normal penalty 1e + 5 Tangential penalty 1e + 2 Tangential penalty increment 2		
Unsymmetric	Symmetric[16]	Symmetric	Unsymmetric	Symmetric[16]	Symmetric
3	3	3	3	3	3
0·737e − 2	0·730e − 2	0·737e − 2	0·737e − 2	0·730e − 2	0·737e − 2
2	2	2	2	2	2
0·209e − 3	0·249e − 3	0·209e − 2	0·341e − 3	0·249e − 3	0·341e − 3
2	2	2	3	5	3
0·155e − 3	0·195e − 3	0·159e − 3	0·106e − 3	0·476e − 2	0·120e − 3
2	3	2	3	4	3
0·487e − 4	0·144e − 3	0·515e − 4	0·345e − 4	0·215e − 2	0·320e − 4
2	2	2	2	2	2
0·236e − 4	0·530e − 4	0·212e − 4	0·179e − 4	0·130e − 3	0·177e − 4
2	2	2	4	2	4
0·137e − 4	0·253e − 4	0·129e − 4	0·923e − 5	0·544e − 4	0·918e − 5
2	2	2	4	3	4
0·108e − 4	0·145e − 4	0·105e − 4	0·466e − 5	0·403e − 4	0·469e − 5
2	2	2	4	2	4
0·717e − 5	0·108e − 4	0·723e − 5	0·146e − 5	0·325e − 4	0·148e − 5
2	2	2	2	4	2
0·661e − 5	0·736e − 5	0·649e − 5	0·274e − 6	0·914e − 5	0·271e − 6
2	2	2	2	4	2
0·590e − 5	0·664e − 5	0·593e − 5	0·699e − 7	0·445e − 5	0·773e − 7
2	2	2	2	4	2
0·329e − 5	0·582e − 5	0·336e − 5	0·153e − 7	0·140e − 5	0·185e − 7
2	2	2	2	2	2
0·308e − 5	0·337e − 5	0·302e − 5	0·326e − 8	0·276e − 6	0·324e − 8
2	2	2	2	2	2
0·289e − 5	0·309e − 5	0·288e − 5	0·694e − 9	0·700e − 6	0·648e − 9
2	2	2	2	2	2
0·272e − 5	0·289e − 5	0·272e − 5	0·148e − 9	0·149e − 7	0·108e − 9
2	2	2	2	2	2
0·255e − 5	0·272e − 5	0·255e − 5	0·315e − 10	0·313e − 8	0·281e − 10
2	2	2	—	2	—
0·239e − 5	0·255e − 5	0·239e − 5	—	0·658e − 9	—
2	2	2	—	2	—
0·224e − 5	0·239e − 5	0·225e − 5	—	0·138e − 9	—
2	2	2	—	2	—
0·211e − 5	0·225e − 5	0·211e − 5	—	0·291e − 10	—
2	2	2	—	—	—
0·127e − 5	0·211e − 5	0·130e − 5	—	—	—
—	2	—	—	—	—
—	0·124e − 5	—	—	—	—
Tot. iteration					
39	42	39	39	49	39

Table V. Residual of constraints and number of iterations for test no. 7

Penalty 1e + 4 no increment	Penalty 1e + 5 no increment	Penalty 1e + 6 no increment	Penalty 1e + 4 increment 10	Penalty 1e + 5 increment 10	Penalty 1e + 6 increment 10
2	2	2	2	2	2
0·296e + 5	0·309e + 4	0·310e + 3	0·296e + 5	0·309e + 4	0·310e + 3
2	2	2	2	2	2
0·141e + 4	0·154e + 2	0·155e + 0	0·147e + 3	0·154e + 1	0·155e − 1
2	2	2	2	2	2
0·671e + 2	0·765e − 1	0·772e − 4	0·732e + 0	0·771e − 3	0·768e − 6
2	2	2	2	2	2
0·319e + 1	0·380e − 3	0·386e − 7	0·364e − 2	0·385e − 6	0·381e − 10
2	2	2	2	2	1
0·152e + 0	0·189e − 5	0·192e − 10	0·181e − 4	0·192e − 9	0·379e − 10
2	2	1	2	1	1
0·724e − 2	0·941e − 8	0·192e − 10	0·901e − 7	0·192e − 9	0·270e − 12
2	1	1	2	1	—
0·345e − 3	0·941e − 8	0·451e − 13	0·448e − 9	0·103e − 12	—
2	1	—	1	—	—
0·164e − 4	0·461e − 10	—	0·448e − 9	—	—
2	—	—	1	—	—
0·782e − 6	—	—	0·186e − 11	—	—
2	—	—	—	—	—
0·372e − 7	—	—	—	—	—
1	—	—	—	—	—
0·372e − 7	—	—	—	—	—
1	—	—	—	—	—
0·177e − 8	—	—	—	—	—
Tot. iterations					
22	14	12	16	12	10

phase can be deduced by comparing results collected in Table VI. The symmetrization technique proposed in Reference 16 has also been tried, but no convergence has been achieved. This occurs because the problem is very sensitive to the contact force variations. The jump of the tangential force at the first augmentation causes numerical oscillations and divergence of the solution when the solution shifts from the frictionless to the frictional state.

Other tests carried out using realistic material and contact parameters of steel have shown the same trend. Examples with thermal coupling have shown a small influence on the convergence rate. This is due to the fact that ill-conditioning problems are mainly due to the mechanical field.

CONCLUSIONS

A technique to symmetrize a thermomechanical contact problem is presented. Symmetrization and augmentation are combined in a suitable way to permit good rates of convergence and to avoid ill-conditioning of the global stiffness matrices. The effectiveness of penalty updates has also been shown. The methods have been applied to different problems with linear geometry. However, from the theoretical point of view no further difficulties are involved when using the proposed method in a fully non-linear formulation.

Table VI. Residual of constraints and number of iterations for test no. 8

Normal penalty 1e + 9 Tangential penalty 1e + 4		Normal penalty 1e + 9 Tangential penalty 1e + 6	
Unsymmetric	Symmetric	Unsymmetric	Symmetric
5	5	4	4
0·296e + 4	0·296e + 4	0·301e + 2	0·302e + 2
5	5	5	5
0·145e + 3	0·145e + 3	0·228e + 1	0·225e − 1
3	3	2	2
0·291e + 2	0·419e + 2	0·675e − 1	0·216e + 0
3	3	2	2
0·682e + 1	0·913e + 1	0·675e − 4	0·158e − 1
2	2	2	2
0·188e + 1	0·218e + 1	0·263e − 6	0·466e − 2
2	2	2	2
0·567e + 0	0·633e + 0	0·117e − 8	0·604e − 3
2	2	1	2
0·177e + 0	0·200e + 0	0·117e − 8	0·605e − 4
2	2	1	2
0·561e − 1	0·635e − 1	0·845e − 11	0·153e − 4
2	2	—	2
0·178e − 1	0·201e − 1	—	0·314e − 6
2	2	—	2
0·567e − 2	0·640e − 2	—	0·322e − 6
2	2	—	2
0·180e − 2	0·204e − 2	—	0·138e − 7
2	2	—	2
0·574e − 3	0·648e − 3	—	0·573e − 8
2	2	—	2
0·182e − 3	0·206e − 3	—	0·612e − 9
2	2	—	2
0·582e − 4	0·656e − 4	—	0·801e − 10
2	2	—	—
0·185e − 4	0·209e − 4	—	—
2	2	—	—
0·589e − 5	0·664e − 5	—	—
2	2	—	—
0·188e − 5	0·211e − 5	—	—
2	2	—	—
0·597e − 6	0·673e − 6	—	—
2	2	—	—
0·190e − 6	0·214e − 6	—	—
2	2	—	—
0·605e − 7	0·681e − 7	—	—
Tot. iterations			
48	48	19	33

REFERENCES

1. T. Belytschko and O. M. Neal, 'The vectorized pinball contact impact routine', *Transl. 10th Int. Conf. on Structural Mechanics in Reactor Technology*, Anaheim, CA, August 1989.

2. A. R. Johnson and C. J. Quigley, 'Frictionless geometrically non-linear contact using quadratic programming', *Int. j. numer. methods eng.*, **28**, 127–144 (1989).
3. J. W. Ju and R. L. Taylor, 'A perturbed lagrangian formulation for the finite element solution of nonlinear frictional contact problems', *J. Theoret. Appl. Mech.* (Suppl.), **7**, 1–14 (1988).
4. K. J. Bathe and A. Chaudhary, 'A solution method for planar and axisymmetric contact problems', *Int. j. numer. methods eng.*, **21**, 65–88 (1985).
5. G. Zavarise, Problemi termomeccanici di contatto — aspetti fisici e computazionali, *Ph.D. Thesis*, Ist. di Sciencza e Tecnica delle Costruzioni, Univ. of Padua, Italy, 1991.
6. G. Zavarise, P. Wriggers, E. Stein and B. A. Schrefler, 'Real contact mechanisms and finite element formulation — a coupled thermomechanical approach', *Int. j. numer. methods eng.*, **35**, 767–785 (1992).
7. B. Schrefler and G. Zavarise, 'Constitutive laws for normal stiffness and thermal resistance on contact element', *Microcomput. Civil Eng.*, **8**, 299–308 (1993).
8. P. Wriggers and J. C. Simo, 'A note on tangent stiffness for fully nonlinear contact problems', *Comm. appl. numer. methods*, **1**, 199–203 (1985).
9. G. Zavarise, B. A. Schrefler and P. Wriggers, 'Consistent formulation for thermomechanical contact based on microscopic interface laws', *Proc. COMPLASS III, 3rd Int. Conf. on Computational Plasticity*, Barcelona, Spain, April 1992.
10. P. Wriggers and G. Zavarise, 'Application of augmented lagrangian techniques for non-linear constitutive laws in contact interface', *Comm. appl. numer. methods eng.*, **9**, 815–824 (1993).
11. D. P. Bertsekas, *Constrained Optimization and Lagrange Multiplier Methods*, Academic Press, New York, 1984.
12. P. Wriggers, J. C. Simo and R. L. Taylor, 'Penalty and augmented lagrangian formulation for contact problems', in J. Middleton and G. N. Pande (eds.), *Proc. NUMETA Conf.*, Balkema, Rotterdam, 1985.
13. P. Wriggers, T. Vu Van and E. Stein, 'Finite element formulation of large deformation impact–contact problems with friciton', *Comput. Struct.*, **37**, 319–331 (1990).
14. N. Kikuchi and J. T. Oden, *Contact Problems in Elasticity: A Study of Variational Inequalities and Finite Element Methods*, SIAM, Philadelphia, 1988.
15. J. C. Simo and T. A. Laursen, 'An augmented lagrangian treatment of contact problems involving friciton', *Comput. Methods Appl. Mech. Eng.*, to appear.
16. T. A. Laursen and J. C. Simo, 'Algorithmic symmetrization of Coulomb frictional problems using augmented lagrangians', *Comput. Methods Appl. Mech. Eng.*, to appear.
17. P. Wriggers and C. Miehe, 'On the treatment of contact constraints within coupled thermomechanical analysis', *Comput. Methods Appl. Mech. Eng.*, to appear.
18. G. Zavarise and B. A. Schrefler, 'Simulation of thermomechanical contact problems', in F. Maceri and G. Iazeolla (eds.), *Proc. of EUROSIM '92 Simulation Congr.*, Capri, 1992.
19. P. Wriggers and G. Zavarise, 'Thermomechanical contact — a rigorous but simple numerical approach', *Comput. Struct.*, **46**, 47–53 (1993).
20. O. C. Zienkiewicz and R. L. Taylor, *The Finite Element Method*, 4th edn, McGraw-Hill, London, 1989.
21. J. T. Oden and E. B. Pires, 'Nonlocal and nonlinear friction laws and variational principles for contact problems in elasticity', *J. Appl. Mech. ASME*, **50**, 67–76 (1983).
22. S. Song and M. M. Yovanovich, 'Explicit relative contact pressure expression: dependence upon surface roughness parameters and Vickers microhardness coefficients', *AIAA '87 25th Aerospace Sciences Meeting, Paper No. 87-0152*, Reno, Nevada, 1987.
23. B. Nour-Omid and P. Wriggers, 'A note on the optimum choice for penalty parameters' *Comm. appl. numer. methods*, **3**, 581–585 (1987).